Fluid Structure Interaction Analyses of Tidal Turbines

Joseph Banks, Kutalmis Bercin, Thomas P. Lloyd, Stephen R. Turnock
Faculty of Engineering and the Environment, University of Southampton, Southampton, SO17 1BJ. UK.
E-mail: {J.Banks; K.Bercin; T.P.Lloyd; S.R.Turnock}@soton.ac.uk

I. Introduction

Horizontal axis tidal turbines (HATTs) must provide reliable electrical energy production in a subsea environment with minimal maintenance. Failures related to turbine blades will have a significant impact on their overall cost-effectiveness. The use of composite blades for such devices offers mass and cost savings [1], [2], however to fully utilise this benefit blades have to be designed to be more flexible than traditional blades. Hence it is important that the fluid structure interaction (FSI) of the blades is well understood. In its simplest form this allows the performance of a turbine blade to be assessed in it deformed state. Composite materials also create the possibility of blades that deform into different optimised shapes for different load conditions [2]. This could maximise the turbine efficiency over a broader range of the tidal cycle. To achieve this the interaction between the fluid loading and the structural response needs to be considered within the design process.

HATTs operate in a highly unsteady environment due to large fluctuating velocities caused by the oceanic turbulent boundary layer. This results in a dynamic interaction of the hydrodynamic blade loading and its structural response with implications for the assessment of device efficiency and through-life fatigue loading. The coupling of a stochastic flow regime with flapwise and twist deformations of the blade requires fully coupled hydrodynamic and structural simulation of the blade to deal with the inherent non-linearities.

Turbine blade modelling methods are essentially made of three components: hydrodynamics of the flow regime around and through the machine; structural dynamics of the blades and the interaction of these two mechanisms [3]. Hydrodynamic loading applied to the blade can be assessed using a number of methods, such as BEM, actuator line and CFD methods. Similarly, a number of approaches can be used to assess the structural response of the blades. These include bean modal decomposition (beam theory), multi-body and finite element methods. Coupling the hydrodynamic and structural solutions can be achieved in an iterative manner (two-way), where the fluid and structural convergence simultaneously, or quasi-steady (one-way), where the converged fluid loadings are applied to the structural model.

Computational cost increases for higher fidelity simulations. Hence the size of the problem in terms of number of grid cells and time steps required influences the choice of simulation approach. For example, BEM theory can be used to represent turbine arrays inside a CFD simulation [4]. More recently a beam theory structural solver has been included into this method allowing both static and dynamic structural deformations to gust loading to be analysed [3]. This approach allows dynamic simulations of fluid structure interactions of devices in an efficient way; however as only the blade twist in included in the assessment of the deformed blades' performance this will come at the expense of physics fidelity. In contrast detailed simulations of the hydrodynamic loading on a tidal turbine in a turbulent flow have been performed using large eddy simulation (LES) [5]. This comes at a considerable computational cost ($\sim 10^4$ CPU hours). If this type of simulation was directly coupled with a finite element analysis of the dynamic structural response the computational cost would likely triple based on the fully coupled analysis of a flapping foil presented in [6]. High fidelity simulations provide the opportunity to assess the limitations and accuracy of simpler, more efficient methods.

This paper aims to take the high fidelity fluid loading obtained in [5] and apply a static structural response using the beam theory adopted by [3]. The same test case is also simulated using the coupled BEM-beam theory approach. This allows the impact of flapwise deflections and fluid solver fidelity to be assessed on the fluid structure analysis of the thrust and power produced by a flexible bladed device.

II. FSI methodology

In this section we outline the computational methodology adopted. Figure 1 shows a flowchart depicting procedure, which involves three computational models: a finite volume fluid dynamics code; a BEM theory code; and an analytical beam theory model. These components are described individually next. A key consideration is that we only consider quasi-static blade deflection in both the LES and BEM approaches. Note that the BEM approach can also be used to assess dynamic FSI [3], although this is not included here.

A. Finite volume method

Simulations were carried out using the OpenFOAM® 2.1.0 libraries, augmented by custom solvers and boundary conditions. Full details of the solver settings are

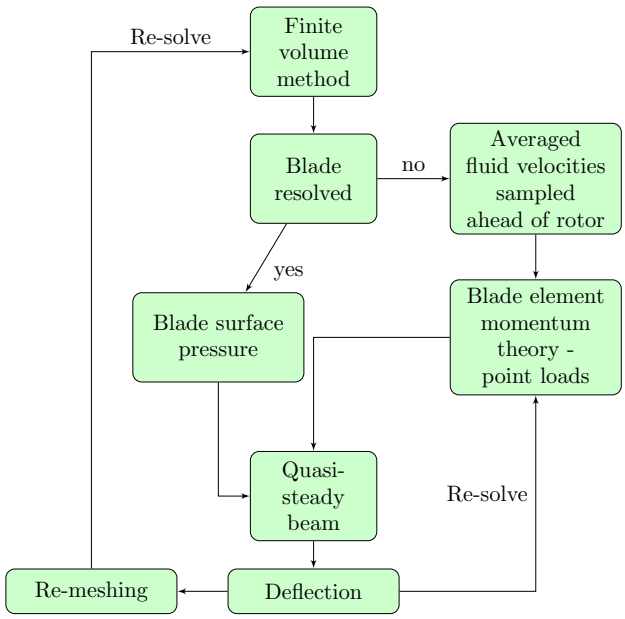

Fig. 1. Flowchart describing fluid structure interaction assessment procedure.

provided by [3] and [5]. When the turbine blades are resolved, the simulation is fully unsteady; that is, rotation is included using a dynamic mesh procedure, with a cylinder surrounding the turbine. Fluxes are interpolated between the grid regions using an *arbitrary mesh interface*. Where OpenFOAM is used to provide velocity data to the BEM code, no explicit rotation is included. Both the filtered (LES) and unsteady Reynolds-averaged (URANS) governing equations are solved, depending on the simulation. LES is used to resolve turbulence. This allows spectra of turbine performance to be derived, based on stochastic fluid loading. The URANS equations can represent low wavenumber unsteady effects, such as low frequency gust, but model the turbulence spectrum.

B. BEM theory code

The modified BEM code was *Cwind*, developed by [7]. The code has been written into C++ for easier integration with OpenFOAM. Improvements to the original code are detailed in [3]. BEM theory is used to estimate the forces exerted on a specified blade geometry. The theory combines momentum theory (i.e. the actuator disk theory) and blade element analysis. The former represents the blade swept area as an infinitely thin disc which alters the axial and tangential momentum of fluid particles passing through. The latter divides the blade into a number of non-interacting sections and estimates forces generated by using its aerodynamic force coefficients for its relative velocity inflow.

Such methods have been used by [8] to investigate the possible differences between the loading prediction capabilities of a sectional BEMT model and a finite element model that maps pressure distribution over an identical wind turbine blade, showing negligible difference with respect to the deflection results.

C. Structural modelling

It is Baumgart's [9] assertion that slender solid body modelling, such as for a tidal turbine blade, with a beam model captures the essential features in comparison to a more complex solid or shell - finite element model. In addition, as is claimed in [10], as far as the mechanical features of a three-dimensional blade can be extracted, a one-dimensional beam model can cope with most structural examinations in a prompt way.

BEM theory and LES provides hydrodynamic loading at discrete locations along the blade span that are located at the centre of each segment. A linear structure is considered for simplicity; therefore, each deflection is computed separately and then summed using superposition. Flapwise and edgewise static deformations are computed as

$$v(x) = -Fx^2(3s - x)/6EI \qquad 0 \leq x \leq s \tag{1a}$$

and

$$v(x) = -Fs^2(3x - s)/6EI \qquad s < x \leq x_{tip} \tag{1b}$$

where x is the location where the deflection is monitored on the beam neutral axis $[m]$, s is the location where point loads is applied $[m]$, $v(x)$ is the deflection $[m]$, F is the force in the direction of deflection [N], E is Young's modulus of the blade element material [Nm^{-2}], I is the area moment of inertia of the blade element's cross section $[m^4]$.

Torsional deflections are computed as

$$\gamma(x) = Mx/GJ \qquad 0 \leq x \leq s \tag{2a}$$

and

$$\gamma(x) = \gamma(s) \qquad s < x \leq x_{tip} \tag{2b}$$

where $\gamma(x)$ is the angle of twist relative to the undeformed configuration $[rad]$, M is the twisting moment [Nm], G is the shear modulus of the material [Nm^{-2}] and J is the polar moment of inertia of the relevant section $[m^4]$. The structural properties of the blade were based on a uniform rectangular beam section, matching the blade thickness and 50 % of the blade chord (at a span location of 70 % of the rotor radius). The blade material was chosen as aluminium, with a Young's Modulus of 70 GPa.

D. Re-meshing

When the blades are resolved in the fluid computation, the corrected turbine performance based on the deflected blade shape is desired. To achieve this, the sectional flapwise, edgewise and torsional deflections are applied to morph the blade geometry file. Morphing is achieved using the in-house *adaptFlexi* tool. The new blade shape is then used to re-mesh the fluid domain. This is relatively simple when using the *snappyHexMesh* utility. The fluid problem is then re-solved to derive adjusted thrust and power coefficients.

III. Test case description

A. Experimental data

The simulated turbine is a model scale device that has been previously tested by [11]. Key parameters are given in Table I.

TABLE I
TEST CASE PARTICULARS.

Symbol	Meaning	Value
R	Rotor radius	0.4 m
B	Number of blades	3
U_0	Mean freestream velocity	1.4 ms^{-1}
Ω	Rotational velocity	20.68 $rads^{-1}$
TSR	Tip speed ratio	5.96
θ_{hub}	Hub twist angle	15°

The tip speed ratio is defined as $TSR = \Omega R/U_0$. For this case, the turbine thrust and power coefficients are $C_T = 2T/\rho A U_0^2 = 1$ and $C_P = 2\Omega Q/\rho A U_0^3 = 0.36$. Here, T is thrust [$kgms^{-2}$], Q torque [kgm^2s^{-2}], ρ_0 the fluid density [1000 kgm^{-3}] and A [m^2] the rotor projected area. The turbine was tested in low turbulence facilities, and hence the results reported here are not directly comparable. The experimental C_T and C_P are used primarily to assess the quality of the simulation grid. It should be noted that introducing inflow turbulence in the numerical simulation has little effect ($< 1\%$) on the mean thrust and power coefficients [12]. A larger effect is observed for the root mean square of these quantities.

B. Domain design

Since the experimental data have been corrected for tunnel blockage effects, an unbounded domain is used for the simulations. The domain has overall dimensions $L_x \times L_y \times L_z = 10D \times 6D \times 6D$, where x,y and z are the streamwise, vertical and horizontal directions (see Figure 2). The inlet is located $3D$ upstream of the turbine rotor plane, which is centred at the domain origin. A cylindrical rotating region of dimensions $L_x \times R = 0.5\ m \times 0.5\ m$ centred at the domain origin encompasses the turbine rotor. Full details of the LES simulations and grid are provided in [5].

Since the grid is not wall-resolved ($y_1^+ \approx 30$), a wall function is used for the subgrid viscosity. y_1^+ is the non-dimensional first cell height based on the friction velocity and kinematic viscosity, and is a measure of how well the viscous sublayer is resolved. Although we were able to generate a wall-resolved ($y_1^+ = 1$) grid, the smaller time step required proved prohibitive in achieving a converged solution within a reasonable computational time. The implication of this modelling assumption will be assessed in the following Sections.

IV. Rigid blade results

Mean performance measures for the two numerical approaches are compared to the experimental values in Table II. Due to the computational efficiency advantage of the BEM code, this method has been used to assess the turbine performance for a range of tip speeds. This data is presented in Figures 3 and 4. Table II reveals some differences between the LES and BEM methods. The thrust coefficient derived from LES is closer to the experimental value than the BEM. However, the power coefficient predicted by BEM is in very good agreement with the experiment. The LES value is $\sim 19\%$ over-predicted. This effect has been attributed to the wall function approach used in the LES, which does not capture separation well; the BEM is based on aerofoil lift and drag data, and therefore includes separation, despite the lower fidelity of this approach.

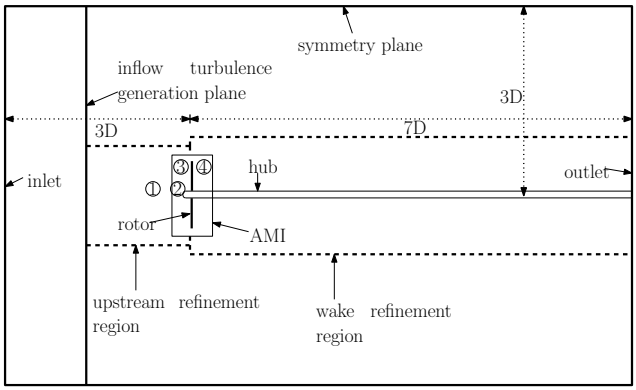

Fig. 2. Schematic representation of simulated case domain.

TABLE II
MEAN EXPERIMENTAL AND NUMERICAL INTEGRAL PERFORMANCE MEASURES.

Coeff.	Exp.	BEM	LES (rigid)	LES (deformed)
$\overline{C}_T$	1.0	0.86	0.98	0.73
$\overline{C}_P$	0.36	0.37	0.43	0.22

Whilst the LES is not suited to providing every data point in Figure 3, it can be used to analyse the time-dependent behaviour of the turbine performance. Samples of the thrust and power coefficients are provided in Figure 6. Large fluctuations in the time traces are evident; these effects cannot be captured by the BEM code.

V. Deformed blade results

The deformed blade shape was calculated using the method outlined in Figure 1, using the mean surface pressure derived from the rigid LES case. Figure 5 shows the deformed shape, where the tip deflection is $\sim 0.035\ m$, or $\sim 9\ \%$ of the turbine radius. Both the edgewise and twist deformations were negligible.

Figures 3 and 4 depict the thrust and power using the quasi-steady beam theory model, coupled with BEM for the full scale turbine presented in [3]. It is evident that FSI effects become more prominent at higher TSRs. The BEM approach allows a rapid assessment of static and dynamic FSI effects (see [3]), however as only the effects of twist

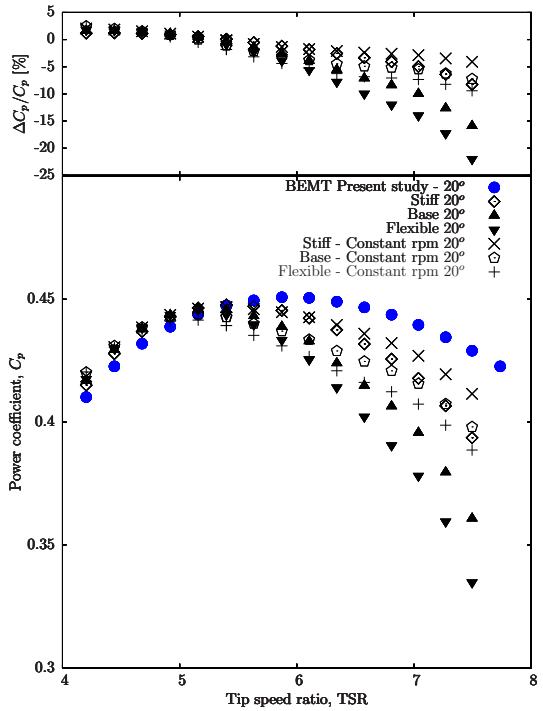

Fig. 3. Power coefficient against tip speed ratio using BEM code. Results shown for both rigid and flexible blades.

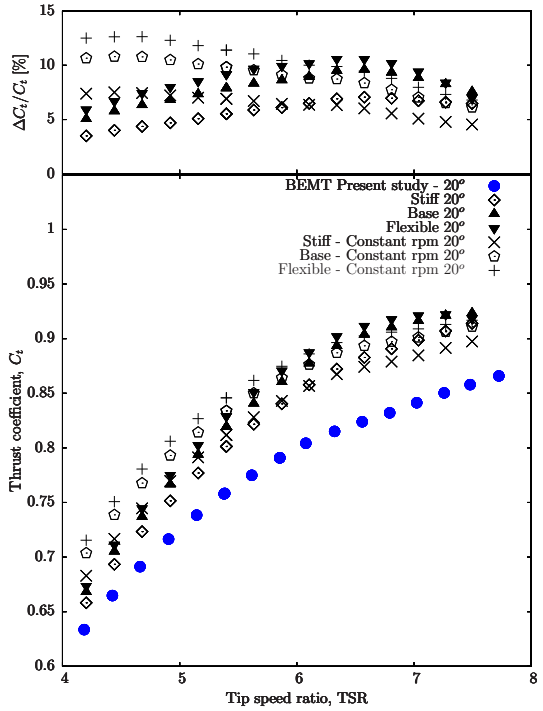

Fig. 4. Thrust coefficient against tip speed ratio using BEM code. Results shown for both rigid and flexible blades.

(a) side (b) end

Fig. 5. Deformed blade shape: rigid (blue); deformed (red).

are currently included in the BEM analysis the significant flap-wise deformation observed in Figure 5 could not be assessed.

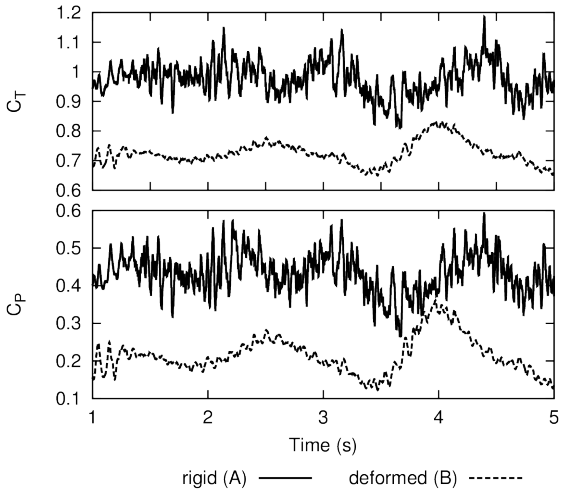

Fig. 6. Time history of turbine thrust and power coefficients derived using LES.

A reduction in power coefficient for a deformed wind turbine blade was also seen by [13]. The authors predicted flapwise deflections similar to those used here. The effect on turbine power was seen to be dependent on TSR, an indication that flow separation is an important effect. For a full scale device ($R = 64\ m$), a reduction in power of $\sim 14\%$ is seen for a TSR of 6, but not at TSR $= 5$.

The LES of the deformed blade geometry revealed a significant decrease in both the thrust and Torque (see Table II). This reduction in the mean values can also be seen in the time history trace in Figure 6. Both the rigid and deformed blade simulations display a similar low frequency fluctuation caused by the turbulent eddies passing through the rotor. However there is a noticeable difference in the high frequency fluctuations; this may be due to an increased amount of upwinding introduced in the deformed case, in order to ensure stability. The reduction in power and thrust for the deformed blade can be seen in the pressure distribution at key blade sections down the blade presented in Figure 7. The pressure coefficient is defined as

$$\overline{C}_{pr} = \frac{2\overline{p}}{\rho_0(U_0^2 + \Omega^2 r^2)}. \tag{3}$$

The reduced magnitude of the pressure difference over the deformed blade reveals a reduction in the blade's performance. Reduced lift would contribute to a reduction in thrust, while increased drag serves to lower the power. This indicates that the operating condition of the blade has been altered by the significant flapwise deformation. The main cause of the performance reduction can be identified as a significant increase in separation along the blade, depicted in Figure 8. The difference between the rigid and deformed cases is easily observed on the blade suction side. There is some separation in the rigid case, but this is restricted to the root area, where the blade geometry has

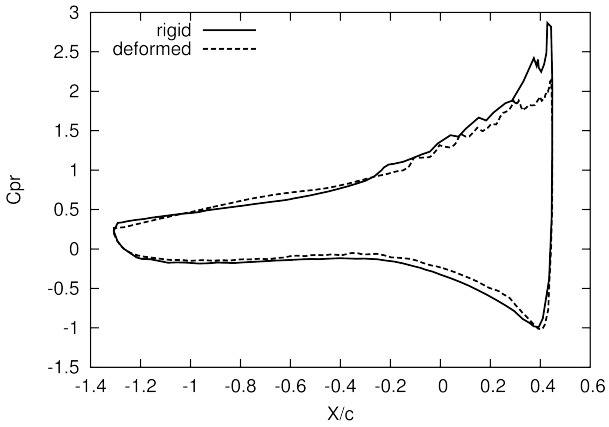

(a) $r/R = 0.35$

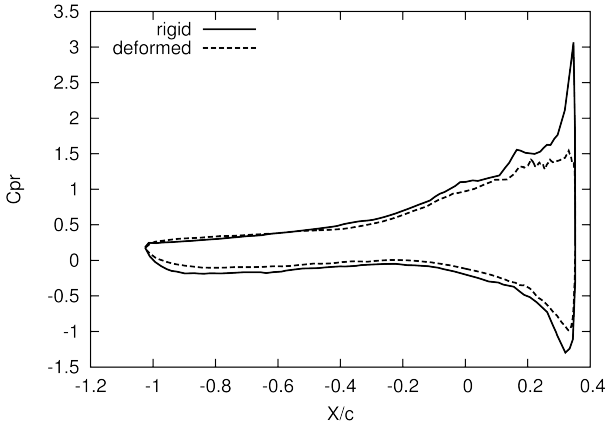

(b) $r/R = 0.6$

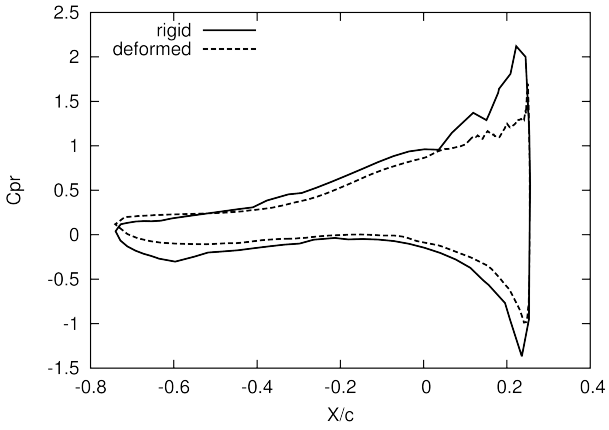

(c) $r/R = 0.85$

Fig. 7. Surface pressure coefficient at three spanwise locations.

(a) Rigid (b) deformed

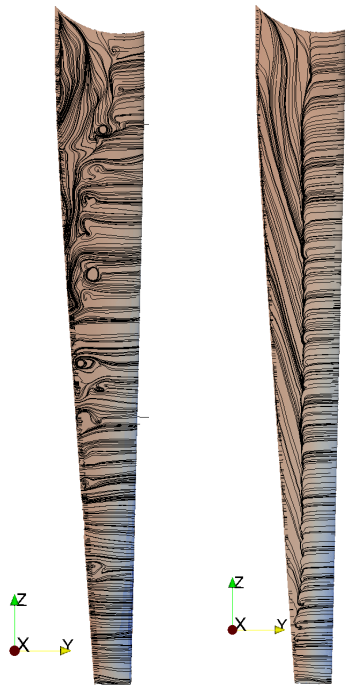

(c) Rigid (d) deformed

Fig. 8. Limiting surface streamlines for rigid and deformed blades: pressure side (top); suction side (bottom).

been simplified. Hence this is not expected to contribute significantly to the turbine power. For the deformed case, the separated region extends along the span almost up to the tip.

The flow pattern revealed in Figure 8 is elucidated by examining the radial velocity. In Figure 9, the blade is aligned with the z axis. It is evident that flow in the separated region is towards the blade tip. This phenomenon is expected to directly contribute to the large reduction in mean power between the rigid and deformed cases, as well as the change in mean thrust.

VI. Conclusions

A comparison between two computational approaches for FSI of tidal turbines has been made: one based on LES; the other on BEM. The results presented concern a quasi-static methodology, where a deformed blade ge-

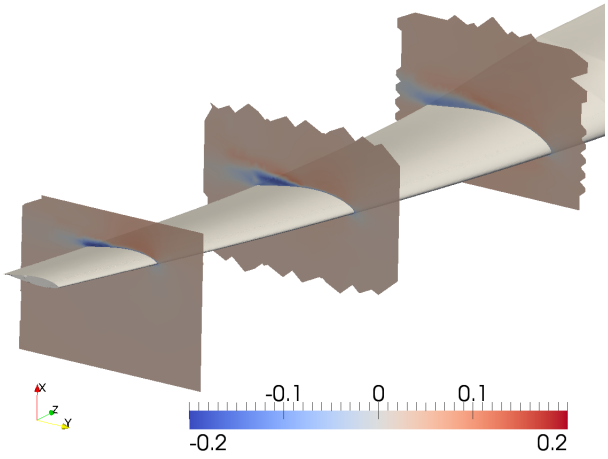

Fig. 9. Slices of mean radial velocity at $r/R = 0.35$, 0.6 and 0.85.

ometry is derived using mean blade loads and a beam theory structural model. This new geometry is then re-meshed and updated performance assessments made using LES. For the chosen case, the hydrodynamic loads are seen to induce minimal twist and edgewise deflection, but large flapwise deflection. The effects of flapwise deflection on performance are not included in BEM. The LES approach offers the ability to investigate this effect, which has not been widely addressed in the literature. A large reduction in power coefficient was observed for the deformed case. This has been linked to increased separation on the deformed blade, which extends over the majority of the blade span. Therefore it is concluded that flapwise deflections can significantly alter the operating condition of a turbine blade and should be included into a FSI BEM analysis.

VII. Acknowledgements

The authors acknowledge the use of the IRIDIS 3/4 High Performance Computing Facility, and associated support services at the University of Southampton. JB and KB gratefully acknowledge funding from the University of Southampton and partial financial support from EPSRC project "Passive adaptive composites" funded through EP/009876/1, and Arup and Partners Ltd. TL wishes to acknowledge the financial support of a University of Southampton Postgraduate Scholarship, dstl and QinetiQ.

References

[1] R. F. Nicholls-Lee and S. R. Turnock, "Enhancing performance of a horizontal axis tidal turbine using adaptive blades," in *OCEANS 2007 - Europe*, USA, 2007, pp. 1–6.

[2] R. F. Nicholls-Lee, S. R. Turnock, and S. W. Boyd, "Application of bend-twist coupled blades for horizontal axis tidal turbines," *Renewable Energy*, vol. 50, pp. 541 – 550, 2013.

[3] K. Bercin, T. Lloyd, Z.-T. Xie, and S. R. Turnock, "Efficient method for analysing fluid-structure interaction of horizontal axis tidal turbine blades," in *Proceedings of the 10th European Wave and Tidal Energy Conference*, 2nd-5th September, Aalborg (to appear), 2013.

[4] S. R. Turnock, A. B. Phillips, J. Banks, and R. Nicholls-Lee, "Modelling tidal current turbine wakes using a coupled rans-bemt approach as a tool for analysing power capture of arrays of turbines," *Ocean Engineering*, vol. 38, no. 11-12, pp. 1300 – 1307, 2011.

[5] T. Lloyd, S. R. Turnock, and V. Humphrey, "Computation of inflow turbulence noise of a tidal turbine," in *Proceedings of the 10th European Wave and Tidal Energy Conference*, 2nd-5th September, Aalborg (to appear), 2013.

[6] A. Feymark, "A large eddy simulation based fluid-structure interaction methodology with application in hydroelasticity," Ph.D. thesis, Chalmers University of Technology, 2013.

[7] M. Barnsley and J. Wellicome, "Dynamic models of wind turbines aerodynamic model development," the Commission of the European Communities Directorate, Tech. Rep. JOUR 0110, 1993.

[8] T. J. Knill, "The application of aeroelastic analysis output load distributions to finite element models of wind," *Wind Engineering*, vol. 29, no. 2, pp. 153–168, 2005.

[9] A. Baumgart, "A mathematical model for wind turbine blades," *Journal of Sound and Vibration*, vol. 251, no. 1, pp. 1 – 12, 2002.

[10] D. J. Malcolm and D. L. Laird, "Modeling of blades as equivalent beams for aeroelastic analysis," in *2003 ASME Wind Energy Symposium AIAA/ASME*, Reno, USA, 2003, pp. 293–303.

[11] A. S. Bahaj, A. F. Molland, J. R. Chaplin, and W. Batten, "Power and thrust measurements of marine current turbines under various hydrodynamic flow conditions in a cavitation tunnel and a towing tank," *Renewable Energy*, vol. 32, no. 3, pp. 407–426, Mar. 2007.

[12] I. Afgan, J. Mcnaughton, D. Apsley, S. Rolfo, and T. Stallard, "Large-eddy simulation of a 3-bladed horizontal axis tidal stream turbine: comparisons to RANS and experiments," in *Proceedings of the 7th International Symposium on Turbulence, Heat and Mass Transfer*, 24th-27th September, Palermo, 2012, pp. 1–13.

[13] D.-h. Kim and Y.-h. Kim, "Performance Prediction of a 5MW Wind Turbine Blade Considering Aeroelastic Effect," *World Academy of Science, Engineering and Technology*, vol. 57, pp. 771–775, 2011.